

# Coherence Peak in the Spin Susceptibility from Nesting in Spin-Triplet Superconductors; A Probe for Line Nodes in $\text{Sr}_2\text{RuO}_4$

Mayumi Yakiyama and Yasumasa Hasegawa

*Department of Material Science,  
Graduate School of Science,  
Himeji Institute of Technology  
Ako, Hyogo 678-1297, Japan*

(Dated: October 29, 2018)

We study the dynamical spin susceptibility  $\chi(\mathbf{q}, \omega)$  for spin-triplet superconductivity. We show that a large peak at  $\omega = 2\Delta$  appears in  $\text{Im}\chi_{zz}(\mathbf{Q}, \omega)$ , where  $z$  is the direction of the  $\mathbf{d}$  vector for triplet pairing, if Fermi surface has a nested part with the nesting vector  $\mathbf{Q}$  and the order parameter is  $+\Delta$  and  $-\Delta$  in this part of the Fermi surface. If there are line nodes in the nested part of the Fermi surface, a peak appears in either  $\text{Im}\chi_{zz}(\mathbf{Q}, \omega)$  or  $\text{Im}\chi_{+-}(\mathbf{Q}, \omega)$ , or both, depending on the perpendicular component of the nesting vector. The comparison with inelastic neutron scattering experiments can determine the position of the line nodes in triplet superconductor  $\text{Sr}_2\text{RuO}_4$ .

PACS numbers: 74.25 Ha, 74.70 Pq, 61.12 Bt

## I. INTRODUCTION

The superconductivity in  $\text{Sr}_2\text{RuO}_4$ <sup>1</sup> has been revealed to be unconventional by many experiments; it is spin-triplet<sup>2,3</sup>, it breaks time-reversal symmetry<sup>4</sup>, and its energy gap has line nodes<sup>5,6,7,8</sup>.

The triplet superconductivity with horizontal line nodes of the energy gap has been proposed<sup>9</sup> to explain these experiments. The absence of the angle dependence of the thermal conductivity within the  $a$ - $b$  plane<sup>10,11</sup> shows that the line nodes run horizontally on the Fermi surface. The angle resolved ultrasound attenuation experiment<sup>7</sup> is compatible with the horizontal line nodes.

The Fermi surface of  $\text{Sr}_2\text{RuO}_4$  consists of three cylindrical surfaces named  $\alpha$ ,  $\beta$  and  $\gamma$ <sup>12,13</sup>, as predicted by the band calculation<sup>14,15</sup>. The hybridization of the  $d_{xz}$  and  $d_{yz}$  orbitals of ruthenium with the  $p_\pi$  orbital of oxygen makes two one-dimensional bands, if the mixing of these bands is neglected. If small mixing is taken into account, we get hole-like  $\alpha$  and electron-like  $\beta$ , but the nesting of the Fermi surfaces survives as predicted<sup>16</sup> and confirmed by the inelastic neutron scattering experiment<sup>17</sup>. The  $\gamma$  surface is constructed by the  $d_{xy}$  orbital of Ruthenium and is two-dimensional.

Nomura and Yamada<sup>19</sup> have studied the two-dimensional three-band Hubbard model in the third-order perturbation theory and obtained that triplet superconductivity is stabilized mainly in the two-dimensional band. They also obtained the line-node-like power-law behavior in the temperature-dependence of the specific heat due to the vertical node-like energy gap in the  $\alpha$  and  $\beta$  bands. In their treatment the momentum dependence of the gap is determined at the transition temperature  $T_c$ . The spin-triplet state such as

$$\mathbf{d}(\mathbf{k}) = \hat{\mathbf{z}}\Delta \sin k_x \sin k_y (\sin k_x + i \sin k_y), \quad (1)$$

or

$$\mathbf{d}(\mathbf{k}) = \hat{\mathbf{z}}\Delta (\cos^2 k_x - \cos^2 k_y) (\sin k_x + i \sin k_y), \quad (2)$$

where  $\mathbf{d}(\mathbf{k})$  is the  $\mathbf{d}$  vector, should be mixed with

$$\hat{\mathbf{z}}\Delta' (\sin k_y + i \sin k_x), \quad (3)$$

or

$$\hat{\mathbf{z}}\Delta' (\sin k_x - i \sin k_y), \quad (4)$$

at  $T < T_c$  and the vertical line nodes will disappear<sup>9,18</sup>.

Zhitomirsky and Rice<sup>18</sup> proposed the mechanism for the horizontal line nodes that while the active band has a full energy gap, the interband proximity effect makes the horizontal line nodes in the passive band. They assumed that the two-dimensional band is active and that the line nodes are in one-dimensional bands.

On the other hand, It has been shown that spin-triplet superconductivity is induced in the quasi-one dimensional bands by the antiferromagnetic spin fluctuation if the antiferromagnetic spin fluctuation is anisotropic in the spin space<sup>20,21</sup>. If this is the case the one-dimensional bands are expected to have a full energy gap and the two-dimensional band has line nodes.

Therefore, the determination of the gap structure is important to understand the mechanism of unconventional superconductivity in  $\text{Sr}_2\text{RuO}_4$ . Bulk measurements such as specific heat, NMR and thermal conductivity cannot distinguish which part of the Fermi surface has the line nodes,  $\alpha$ ,  $\beta$  or  $\gamma$ .

In the inelastic neutron scattering experiments, imaginary part of the dynamical spin susceptibility,  $\text{Im}\chi(\mathbf{q}, \omega)$ , is observed, from which we can get the information of the superconducting order parameter. The so-called 41 meV peak in the spin-singlet  $d$ -wave superconducting state of  $\text{YBa}_2\text{Cu}_3\text{O}_7$ <sup>22,23,24,25,26</sup> has been observed. Many theoretical studies<sup>27,28,29,30,31,32,33,34,35,36,37</sup> have been done to explain the peak structure in inelastic neutron scattering.

Dynamical susceptibility for the spin-triplet superconductivity has been studied theoretically<sup>38,39</sup>. Recently, the resonance peak in  $\text{Im}\chi(\mathbf{q}, \omega)$  is shown to be a sign of the triplet superconductivity<sup>40,41,42</sup>. The order parameter assumed in these papers, however, does not seem to be consistent with experiments in  $\text{Sr}_2\text{RuO}_4$ .

In this paper we show the general form of the dynamical spin susceptibility  $\chi_{ij}(\mathbf{q}, \omega)$  in the unitary states of the triplet superconductivity and calculate it in the system which has the nested Fermi surface with and without line nodes in the nested part of the Fermi surface. We show that the position of the line nodes can be determined by the inelastic neutron scattering experiment, which observes the imaginary part of the dynamical susceptibility<sup>17,43,44</sup>.

## II. DYNAMICAL SPIN SUSCEPTIBILITY OF SPIN-TRIPLET SUPERCONDUCTIVITY

The dynamical spin susceptibility is given by<sup>38,39,40,41</sup>

$$\chi_{ij}^0(\mathbf{q}, i\omega_m) = -\frac{1}{4} \times T \sum_{n, \mathbf{k}} \text{Tr} \left( \hat{\alpha}_i \hat{G}(\mathbf{k}, i\epsilon_n) \hat{\alpha}_j \hat{G}(\mathbf{k} + \mathbf{q}, i\epsilon_n + i\omega_m) \right), \quad (5)$$

where  $\omega_m = 2m\pi T$  and  $\epsilon_n = (2n+1)\pi T$  are Matsubara frequencies ( $m$  and  $n$  are integers), and  $\hat{\alpha}$  and  $\hat{G}(\mathbf{k}, i\epsilon_n)$  are the  $4 \times 4$  Nambu representation of the spin and Green function, respectively, i.e.,

$$\hat{\alpha}_i = \begin{pmatrix} \sigma^i & 0 \\ 0 & \sigma^y \sigma^i \sigma^y \end{pmatrix} = \frac{1 + \rho_z}{2} \sigma^i + \frac{1 - \rho_z}{2} \sigma^y \sigma^i \sigma^y \quad (6)$$

where  $\sigma^i$  ( $i = x, y, \text{ or } z$ ) is a Pauli matrix, and

$$\hat{G}(\mathbf{k}, i\epsilon_n) = \begin{pmatrix} G(\mathbf{k}, i\epsilon_n) & F(\mathbf{k}, i\epsilon_n) \\ F^\dagger(\mathbf{k}, i\epsilon_n) & -G(-\mathbf{k}, -i\epsilon_n) \end{pmatrix}. \quad (7)$$

The  $2 \times 2$  matrix Green function  $G(\mathbf{k}, i\epsilon_n)$  and the anomalous Green function  $F(\mathbf{k}, i\epsilon_n)$  are given as the Fourier coefficients for

$$G_{\alpha, \beta}(\mathbf{k}, \tau) = -\langle T_\tau a_{\mathbf{k}\alpha}(\tau) a_{\mathbf{k}\beta}^\dagger(0) \rangle \quad (8)$$

and

$$F_{\alpha, \beta}(\mathbf{k}, \tau) = \langle T_\tau a_{\mathbf{k}\alpha}(\tau) a_{-\mathbf{k}\beta}(0) \rangle, \quad (9)$$

respectively.

In this paper we consider the weak coupling theory for the spin-triplet superconductivity. We take account of the interaction  $U$  by the random phase approximation (RPA),

$$\chi_{ij}(\mathbf{q}, \omega) = \frac{\chi_{ij}^0(\mathbf{q}, \omega)}{1 - U \chi_{ij}^0(\mathbf{q}, \omega)}, \quad (10)$$

but the essential properties such as a peak in  $\text{Im}\chi_{ii}(\mathbf{q}, \omega)$  is already seen in the absence of the interaction effects.

The order parameter is given by the  $\mathbf{d}$  vector as  $\Delta_{\alpha\beta}(\mathbf{k}) = i((\mathbf{d}(\mathbf{k}) \cdot \boldsymbol{\sigma})\sigma^y)_{\alpha\beta}$ . We study the unitary states,  $\mathbf{d}^*(\mathbf{k}) \times \mathbf{d}(\mathbf{k}) = 0$ , in this paper, since experimental results can be explained by the unitary states. Then we perform the summation over  $n$  in Eq.(5), and get

$$\begin{aligned} \chi_{ij}^0(\mathbf{q}, \omega) &= \frac{1}{4} \sum_{\alpha\alpha'\beta\beta'} \sigma_{\alpha\alpha'}^i \sigma_{\beta\beta'}^j \\ &\times \sum_{\mathbf{k}} \left\{ C_{\alpha\alpha'\beta\beta'}^{(+)}(\mathbf{k}, \mathbf{q}) D^{(-)}(\mathbf{k}, \mathbf{q}, \omega) (f(E_{\mathbf{k}'}) - f(E_{\mathbf{k}})) \right. \\ &\left. + C_{\alpha\alpha'\beta\beta'}^{(-)}(\mathbf{k}, \mathbf{q}) D^{(+)}(\mathbf{k}, \mathbf{q}, \omega) (1 - f(E_{\mathbf{k}'}) - f(E_{\mathbf{k}})) \right\}, \quad (11) \end{aligned}$$

where

$$\begin{aligned} C_{\alpha\alpha'\beta\beta'}^{(\pm)}(\mathbf{k}, \mathbf{q}) &= \frac{\delta_{\alpha\beta'} \delta_{\alpha'\beta}}{2} \\ &\pm \frac{\delta_{\alpha\beta'} \delta_{\alpha'\beta} \xi_{\mathbf{k}} \xi_{\mathbf{k}'} - \text{Re}(\Delta_{\alpha\beta}^*(\mathbf{k}) \Delta_{\alpha'\beta'}(\mathbf{k}'))}{2E_{\mathbf{k}} E_{\mathbf{k}'}} \end{aligned}, \quad (12)$$

$$\begin{aligned} D^{(\pm)}(\mathbf{k}, \mathbf{q}, \omega) &= \frac{1}{E_{\mathbf{k}} \pm E_{\mathbf{k}'} + \omega + i\Gamma} \\ &+ \frac{1}{E_{\mathbf{k}} \pm E_{\mathbf{k}'} - \omega - i\Gamma}, \quad (13) \end{aligned}$$

$\mathbf{k}' = \mathbf{k} + \mathbf{q}$ , and the analytic continuation  $i\omega_m \rightarrow \omega + i\Gamma$  with  $\Gamma \rightarrow +0$  has been done.

We take  $\mathbf{d}$  vector parallel to the  $z$  axis as indicated by experiments<sup>2,3</sup>, to obtain  $\chi_{ij}^0 = 0$  for  $i \neq j$  and

$$\begin{aligned} \chi_{ii}^0(\mathbf{q}, \omega) &= \frac{1}{2} \sum_{\mathbf{k}} \left\{ \tilde{C}_{ii}^{(+)}(\mathbf{k}, \mathbf{q}) D^{(-)}(\mathbf{k}, \mathbf{q}) (f(E_{\mathbf{k}'}) - f(E_{\mathbf{k}})) \right. \\ &\left. + \tilde{C}_{ii}^{(-)}(\mathbf{k}, \mathbf{q}) D^{(+)}(\mathbf{k}, \mathbf{q}) (1 - f(E_{\mathbf{k}'}) - f(E_{\mathbf{k}})) \right\}, \quad (14) \end{aligned}$$

where

$$\begin{aligned} \tilde{C}_{xx}^{(\pm)}(\mathbf{k}, \mathbf{q}) &= \tilde{C}_{yy}^{(\pm)}(\mathbf{k}, \mathbf{q}) = \tilde{C}_{+-}^{(\pm)}(\mathbf{k}, \mathbf{q}) \\ &= \frac{1}{2} \pm \frac{\xi_{\mathbf{k}} \xi_{\mathbf{k}'} - \text{Re}(d_z^*(\mathbf{k}) d_z(\mathbf{k}'))}{2E_{\mathbf{k}} E_{\mathbf{k}'}} \end{aligned}, \quad (15)$$

and

$$\tilde{C}_{zz}^{(\pm)}(\mathbf{k}, \mathbf{q}) = \frac{1}{2} \pm \frac{\xi_{\mathbf{k}} \xi_{\mathbf{k}'} + \text{Re}(d_z^*(\mathbf{k}) d_z(\mathbf{k}'))}{2E_{\mathbf{k}} E_{\mathbf{k}'}}. \quad (16)$$

Depending on the sign of  $\text{Re}(d_z^*(\mathbf{k}) d_z(\mathbf{k}'))$  in the coherence factor,  $\tilde{C}_{ii}^{(-)}$  in Eqs. (15) and (16), a peak will appear in either  $\text{Im}\chi_{+-}(\mathbf{q}, \omega)$  or  $\text{Im}\chi_{zz}(\mathbf{q}, \omega)$ , i.e. if  $\text{Re}(d_z^*(\mathbf{k}) d_z(\mathbf{k}')) > 0$  ( $< 0$ ), a coherence peak appears in  $\chi_{+-}(\mathbf{q}, \omega)$  ( $\chi_{zz}(\mathbf{q}, \omega)$ ), as we will show in the next section.

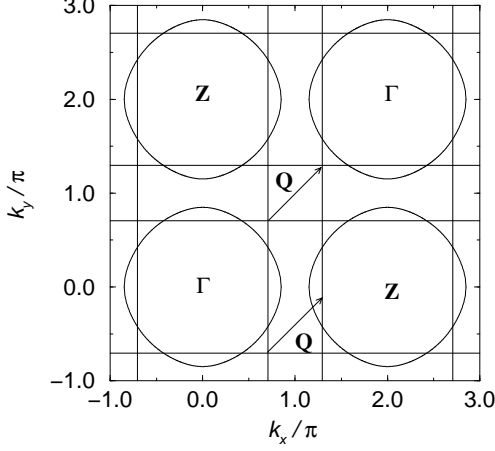


FIG. 1: Fermi surface at  $k_z = 0$  and the nesting vector  $\mathbf{Q}$ .

### III. COHERENCE PEAK FROM THE NESTED FERMI SURFACE

In order to study the coherence peak in  $\text{Sr}_2\text{RuO}_4$ , we take the simple three-band model, where there are two one-dimensional bands and a two-dimensional band, i.e.,

$$\epsilon_{\mathbf{k}}^{(1)} = -2t_1 \cos(k_x) + \epsilon_{01} \quad (17)$$

$$\epsilon_{\mathbf{k}}^{(2)} = -2t_1 \cos(k_y) + \epsilon_{01} \quad (18)$$

$$\epsilon_{\mathbf{k}}^{(3)} = -2t_3(\cos(k_x) + \cos(k_y)) - 4t'_3 \cos(k_x) \cos(k_y) + \epsilon_{03}, \quad (19)$$

where the lattice constant is taken to be 1. We set parameters as  $t_1 = 0.31$  eV,  $\epsilon_{01} = -0.24$  eV,  $t_3 = 0.44$  eV,  $t'_3 = 0.14$  eV and  $\epsilon_{03} = -0.14$  eV. The Fermi surface is shown in Fig. 1. We set the wave vector  $\mathbf{q}$  to be the nesting vector  $\mathbf{Q}$ . The  $z$  component of  $\mathbf{Q}$  is arbitrary if  $\mathbf{d}(\mathbf{k})$  does not depend on  $k_z$ . Since  $\text{Im}\chi_{ii}^0(\mathbf{Q}, \omega)$  is dominated by the contribution from the one dimensional bands, we consider the dynamical spin-susceptibility only for the one-dimensional bands in this paper.

For the normal state with perfectly nested Fermi surface ( $\xi_{\mathbf{k}'} = -\xi_{\mathbf{k}}$ ) the imaginary part of the dynamical susceptibility is

$$\text{Im}\chi_{\text{normal}}^0(\mathbf{Q}, \omega) = \frac{\pi}{2} N(0) \left( 1 - 2f\left(\frac{\omega}{2}\right) \right), \quad (20)$$

where  $f(\omega/2)$  is the Fermi distribution function and the constant density of states  $N(0)$  is assumed.

We study three possible cases for the triplet superconductivity. In the first case (case A) the constant energy gap opens in the one-dimensional bands, while the line nodes are in the two-dimensional band. In the second case (case B) we assume that the order parameter in the one-dimensional bands depends only on  $k_z$  as  $\cos k_z$ . In the last case (case C) the order parameter in the one-dimensional bands depends both on  $k_y$  and  $k_z$  and it is zero in the horizontal line nodes.

#### A. case A

First we study the case A, where we take the order parameters as

$$d_{1z}(\mathbf{k}) = \Delta_1 \sin k_x \quad (21)$$

$$d_{2z}(\mathbf{k}) = i\Delta_1 \sin k_y, \quad (22)$$

and

$$d_{3z}(\mathbf{k}) = \Delta_3 \left( \sin \frac{k_x}{2} \cos \frac{k_x}{2} + i \cos \frac{k_x}{2} \sin \frac{k_y}{2} \right) \times \cos \frac{k_z}{2}. \quad (23)$$

In the case A, Cooper pairs are formed between the electrons on the nearest sites in the conducting plane ( $\mathbf{r}_i$  and  $\mathbf{r}_i + (\pm a, 0, 0)$ ,  $\mathbf{r}_i + (0, \pm a, 0)$ ) for the one-dimensional electrons, and Cooper pairs are formed between the electrons on  $\mathbf{r}_i$  and  $\mathbf{r}_i + (\pm a/2, \pm b/2, \pm c/2)$  for the two-dimensional electrons. These order parameters can be realized if the pairing Hamiltonian is taken as<sup>18</sup>

$$\begin{aligned} \mathcal{H}' = & \sum_{\mathbf{k}, \mathbf{k}', \sigma, \sigma'} \left( g_{11} \left\{ \sin k_x \sin k'_x a_{\mathbf{k}\sigma}^\dagger a_{-\mathbf{k}-\sigma}^\dagger a_{-\mathbf{k}'-\sigma'} a_{\mathbf{k}\sigma'} \right. \right. \\ & + \left. \sin k_y \sin k'_y b_{\mathbf{k}\sigma}^\dagger b_{-\mathbf{k}-\sigma}^\dagger b_{-\mathbf{k}'-\sigma'} b_{\mathbf{k}\sigma'} \right\} \\ & + g_{13} \left\{ \sin k_x \sin \frac{k'_x}{2} \cos \frac{k'_y}{2} \cos \frac{k'_z}{2} \right. \\ & \times \left. (a_{\mathbf{k}\sigma}^\dagger a_{-\mathbf{k}-\sigma}^\dagger c_{-\mathbf{k}'-\sigma'} c_{\mathbf{k}'\sigma'} + h.c.) \right. \\ & + \left. \sin k_y \cos \frac{k'_x}{2} \sin \frac{k'_y}{2} \cos \frac{k'_z}{2} \right. \\ & \times \left. (b_{\mathbf{k}\sigma}^\dagger b_{-\mathbf{k}-\sigma}^\dagger c_{-\mathbf{k}'-\sigma'} c_{\mathbf{k}'\sigma'} + h.c.) \right\} \Bigg), \quad (24) \end{aligned}$$

where  $a_{\mathbf{k}\sigma}^\dagger$  and  $b_{\mathbf{k}\sigma}^\dagger$  are creation operators for the electron in one-dimensional bands and  $c_{\mathbf{k}\sigma}^\dagger$  is the creation operator for the two-dimensional band. In the above only terms relevant to the spin-triplet superconductivity with  $\mathbf{d}(\mathbf{k}) \parallel \hat{\mathbf{z}}$  are included. The terms proportional to  $g_{11}$  describe the attractive interaction between electrons with up and down spins in the one-dimensional bands which makes the triplet superconductivity with  $\mathbf{d}$  vector parallel to the  $z$  axis. The  $g_{13}$  terms represent the pair hoppings between one-dimensional and two-dimensional Fermi surface.

In this case  $\text{Im}\chi_{ii}^0(\mathbf{Q}, \omega)$  from the one-dimensional band is obtained as

$$\text{Im}\chi_{zz}^0(\mathbf{Q}, \omega) = \begin{cases} 0 & \text{if } \omega < 2\Delta \\ \frac{\pi}{2} N(0) \frac{\omega}{\sqrt{\omega^2 - (2\Delta)^2}} \tanh \frac{\omega}{4T} & \text{if } \omega \geq 2\Delta \end{cases} \quad (25)$$

$$\text{Im}\chi_{+-}^0(\mathbf{Q}, \omega) = \begin{cases} 0 & \text{if } \omega < 2\Delta \\ \frac{\pi}{2} N(0) \frac{\sqrt{\omega^2 - (2\Delta)^2}}{\omega} \tanh \frac{\omega}{4T} & \text{if } \omega \geq 2\Delta \end{cases}, \quad (26)$$

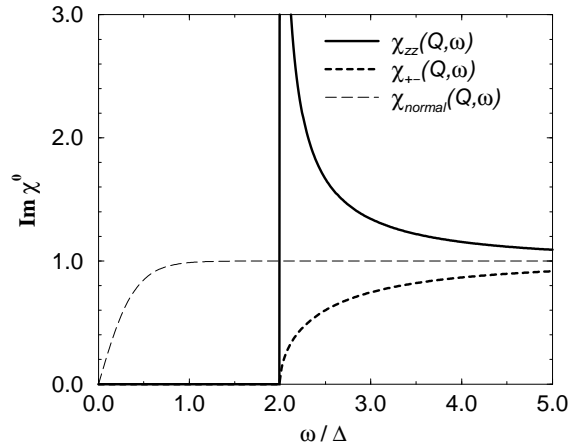


FIG. 2: Imaginary part of the dynamical susceptibility normalized by  $(\pi/2)N(0)$  in case A (full gap on one-dimensional Fermi surface, eqs. (21) and (22)). We take  $T = 0$  for the superconducting state and we take finite  $T$  for the normal state. (Since  $\omega$  and  $T$  is scaled by  $\Delta$ , we take  $T = 0.1\Delta$  for the normal state.)

where  $\Delta = \Delta_1 \sin k_F$  is the energy gap on the Fermi surface in the one-dimensional bands. In Fig. 2 we plot imaginary part of the dynamical susceptibility normalized by  $(\pi/2)N(0)$  as a function of  $\omega$  at  $T = 0$  for the superconducting state and at a finite temperature for the normal state ( $T = 0.1\Delta$ ). Since the coherence factor  $\tilde{C}_{zz}^{(-)}(\mathbf{k}, \mathbf{Q})$  is 1,  $\text{Im}\chi_{zz}^0(\mathbf{Q}, \omega)$  diverges at  $\omega = 2\Delta$  as the density of states in the  $s$ -wave superconductivity.

In Fig. 3 we plot the dynamical susceptibility obtained in RPA with parameters,  $\Delta_1 = 0.001$  eV,  $T = 0.0001$  eV,  $\Gamma = 0.0001$  eV and  $U = 0.175$  eV for the one-dimensional band (Eq. (17) and  $\sin k_F \approx 0.922$ ). A peak appears at  $\omega = 2\Delta_1 \sin k_F \approx 0.00184$  eV only in  $\text{Im}\chi_{zz}(\mathbf{Q}, \omega)$ .

### B. case B

Next we study the case B. We assume horizontal line nodes on the one-dimensional Fermi surface as

$$d_{1z}(\mathbf{k}) = \Delta_1 \sin k_x \cos k_z \quad (27)$$

$$d_{2z}(\mathbf{k}) = i\Delta_1 \sin k_y \cos k_z \quad (28)$$

In this case the Cooper pairs in the one-dimensional bands are formed between electrons on  $\mathbf{r}$  and  $\mathbf{r} + (0, 0, \pm c)$ . Although this order parameter is not likely to be realized in  $\text{Sr}_2\text{RuO}_4$ , we study this case to show the mechanism of resonance peak. In this case if we take  $Q_z = 0$  or  $\pi$ , line nodes are connected by  $\mathbf{Q}$  as shown in Fig. 4. For  $Q_z = 0$  we obtain that

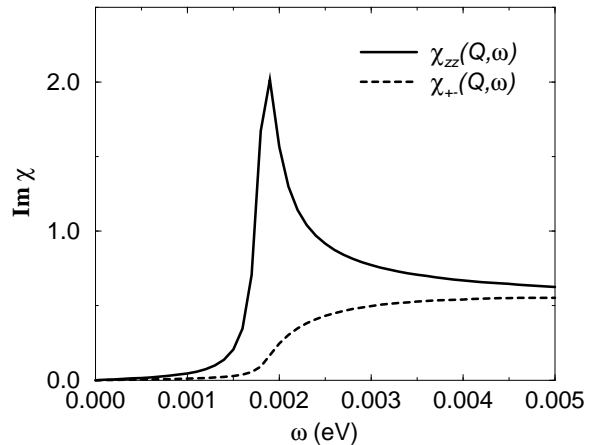


FIG. 3: Imaginary part of the dynamical susceptibility in case A (full gap on one-dimensional Fermi surface, eqs. (21) and (22)) calculated in RPA. We take  $\Delta_1 = 0.001$  eV,  $T = 0.0001$  eV,  $\Gamma = 0.0001$  eV and  $U = 0.175$  eV.

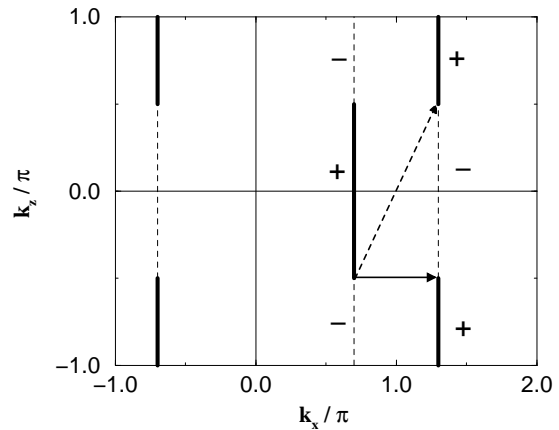


FIG. 4: Nesting vector  $\mathbf{Q}$  in the case B (horizontal line nodes on one-dimensional Fermi surface, eqs. (27) and (28)). Thick solid and thin dashed lines show the side view of the Fermi surface on which order parameter is positive and negative, respectively. Solid arrows ( $Q_z = 0$ ) and dashed arrows ( $Q_z = \pi$ ) are the nesting vectors.

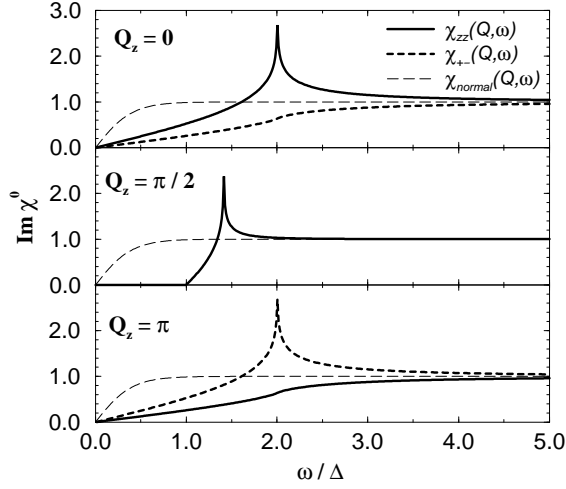


FIG. 5: Imaginary part of the dynamical susceptibility in the case B (line nodes in one-dimensional Fermi surface eqs. (27) and (28)). We take the same parameters as in Fig. 2.

$$\text{Im}\chi_{zz}^0(\mathbf{Q}, \omega) = \begin{cases} N(0)F\left(\arcsin\left(\frac{\omega}{2\Delta}\right) \middle| \left(\frac{2\Delta}{\omega}\right)^2\right) \tanh\frac{\omega}{4T} & \text{if } \omega < 2\Delta \\ N(0)K\left(\left(\frac{2\Delta}{\omega}\right)^2\right) \tanh\frac{\omega}{4T} & \text{if } \omega \geq 2\Delta \end{cases} \quad (29)$$

$$\text{Im}\chi_{+-}^0(\mathbf{Q}, \omega) = \begin{cases} N(0)E\left(\arcsin\left(\frac{\omega}{2\Delta}\right) \middle| \left(\frac{2\Delta}{\omega}\right)^2\right) \tanh\frac{\omega}{4T} & \text{if } \omega < 2\Delta \\ N(0)E\left(\left(\frac{2\Delta}{\omega}\right)^2\right) \tanh\frac{\omega}{4T} & \text{if } \omega \geq 2\Delta \end{cases}, \quad (30)$$

where  $F(\phi|m)$  and  $E(\phi|m)$  are incomplete elliptic integrals of the first and the second kinds, and  $K(m)$  and  $E(m)$  are complete elliptic integrals of the first and second kinds, respectively. As shown in the top panel of Fig. 5,  $\text{Im}\chi_{zz}^0(\mathbf{Q}, \omega)$  diverges at  $\omega = 2\Delta$  as the density of states for superconductivity with line nodes. For  $Q_z = \pi$ ,  $\text{Im}\chi_{zz}^0$  and  $\text{Im}\chi_{+-}^0$  are exchanged.

For  $Q_z = \pi/2$  we get at  $T = 0$

$$\text{Im}\chi_{zz}^0(\mathbf{Q}, \omega) = \text{Im}\chi_{+-}^0(\mathbf{Q}, \omega) = \begin{cases} 0 & \text{if } \omega < \Delta \\ N(0)F\left(\arcsin\left(\left(\frac{\omega}{\Delta}\right)^2 - 1\right) \middle| \frac{1}{((\omega/\Delta)^2 - 1)^2}\right) & \text{if } \Delta \leq \omega < \sqrt{2}\Delta \\ K\left(\frac{1}{((\omega/\Delta)^2 - 1)^2}\right) & \text{if } \omega \geq \sqrt{2}\Delta. \end{cases} \quad (31)$$

In the RPA we get essentially the same result as shown in Fig. 6.

For  $Q_z \neq 0, \pi/2$ , and  $\pi$ ,  $|d_{1z}(\mathbf{k})| + |d_{1z}(\mathbf{k}')|$  at  $k_z = k_F$  has two local maximum of  $2\Delta_1 \sin k_F |\cos(Q_z/2)|$  and

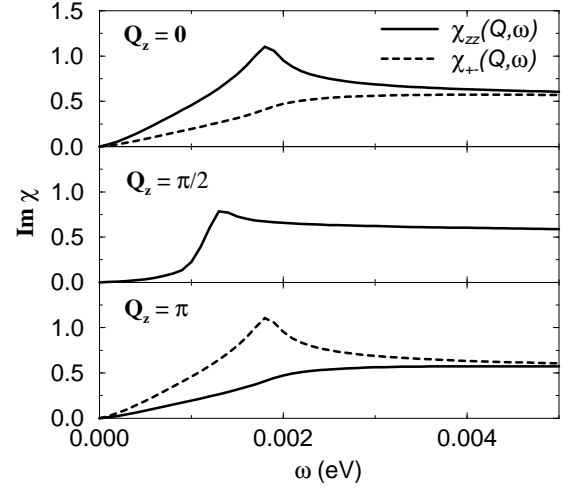


FIG. 6: Imaginary part of the dynamical susceptibility in the case B (line nodes in one-dimensional Fermi surface eqs. (27) and (28)) calculated in RPA. We take the same parameters as in Fig. 3.

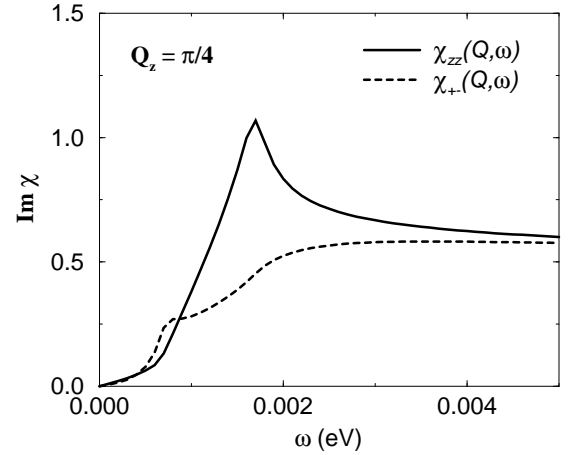


FIG. 7: Imaginary part of the dynamical susceptibility in the case B (line nodes in one-dimensional Fermi surface eqs. (27) and (28)) calculated in RPA. We take the same parameters as in Fig. 3.

$2\Delta_1 \sin k_F |\sin(Q_z/2)|$ . If  $\text{Re}(d_{1z}^*(\mathbf{k})d_{1z}(\mathbf{k}')) > 0$  at  $k_z$ , where  $|d_{1z}(\mathbf{k})| + |d_{1z}(\mathbf{k}')|$  becomes local maximum, then a peak appears in  $\text{Im}\chi_{+-}(\mathbf{Q}, \omega)$ , else a peak appears in  $\text{Im}\chi_{zz}(\mathbf{Q}, \omega)$ . In Fig. 7 we plot the RPA result for  $Q = \pi/4$ . A peak is seen at  $\omega = 2\Delta_1 \cos \pi/8 \approx 0.0017$  in  $\text{Im}\chi_{zz}(\mathbf{Q}, \omega)$  and a small peak is seen at  $\omega = 2\Delta_1 \cos \pi/8 \approx 0.0007$  in  $\text{Im}\chi_{+-}(\mathbf{Q}, \omega)$ .

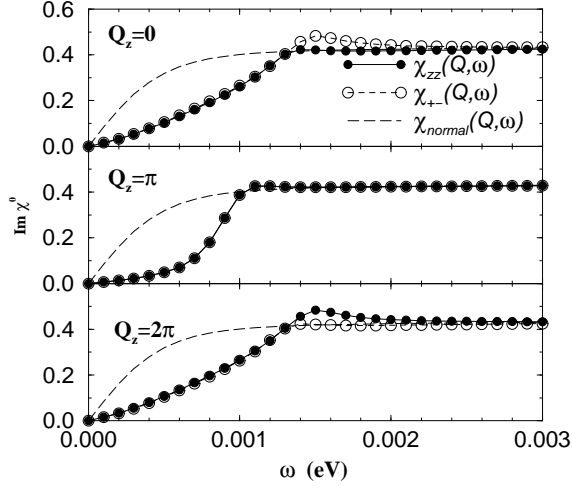


FIG. 8: Imaginary part of the dynamical susceptibility in the case C (line nodes on one-dimensional Fermi surface, eq. (32)). We take  $\Delta_1 = 0.001$  eV,  $T = 0.0001$  eV,  $\Gamma = 0.0001$  eV.

### C. case C

Finally we study the case C. Here we assume the order parameter in the one-dimensional bands to be

$$\begin{aligned} d_{1z}(\mathbf{k}) &= d_{2z}(\mathbf{k}) \\ &= \Delta_1 \left( \sin \frac{k_x}{2} \cos \frac{k_y}{2} + i \cos \frac{k_x}{2} \sin \frac{k_y}{2} \right) \\ &\times \cos \frac{k_z}{2} \end{aligned} \quad (32)$$

This type of superconductivity is realized if the two-dimensional band is active and the one-dimensional bands are passive<sup>18</sup>. In this case the  $\Gamma$  and  $Z$  points in Fig.1 are not equivalent and the order parameter is zero at  $k_z = \pm\pi, \pm 3\pi$ . We calculate  $\text{Im}\chi_{ii}(\mathbf{Q}, \omega)$  numerically and plot  $\text{Im}\chi_{ii}(\mathbf{Q}, \omega)$  as a function of  $\omega$  in Fig. 8. The small coherence peak exists at  $\omega \approx 1.5\Delta_1$ . In this case  $\text{Re}(d_z^*(\mathbf{k})d_z(\mathbf{k} + \mathbf{q}))$  changes sign for  $\mathbf{k}$  on the Fermi surface. The small coherence peak in  $\chi_{+-}(\mathbf{Q}, \omega)$  for  $Q_z = 0$  and that in  $\chi_{zz}(\mathbf{Q}, \omega)$  for  $Q_z = 2\pi$  can be understood as follows. At  $k_x = k_F \approx 0.63\pi$  and  $\mathbf{Q} = (2\pi - 2k_F, 2\pi - 2k_F, Q_z)$ , the maximum value of

$$\begin{aligned} &|d_{1z}(\mathbf{k})| + |d_{1z}(\mathbf{k}')| \\ &= \frac{\Delta_1}{2} \left( \left| \cos \frac{k_z}{2} \sqrt{1 - \cos k_F \cos k_y} \right. \right. \\ &\quad \left. \left. + \left| \cos \frac{k_z + Q_z}{2} \sqrt{1 - \cos k_F \cos(k_y - 2k_F)} \right| \right) \end{aligned} \quad (33)$$

is approximately  $1.52\Delta_1$  at  $k_y \approx 1.62\pi$  and  $k_z = 0$ , if  $Q_z = 0$  or  $2\pi$ . Since  $\text{Re}(d_{1z}^*(\mathbf{k})d_{1z}(\mathbf{k}')) > 0$  ( $< 0$ ) at  $k_y \approx 1.62\pi$  and  $k_z = 0$  for  $Q_z = 0$  ( $Q_z = 2\pi$ ),  $\text{Im}\chi_{+-}(\mathbf{Q}, \omega)$  has a peak at  $\omega \approx 1.52\Delta_1$ .

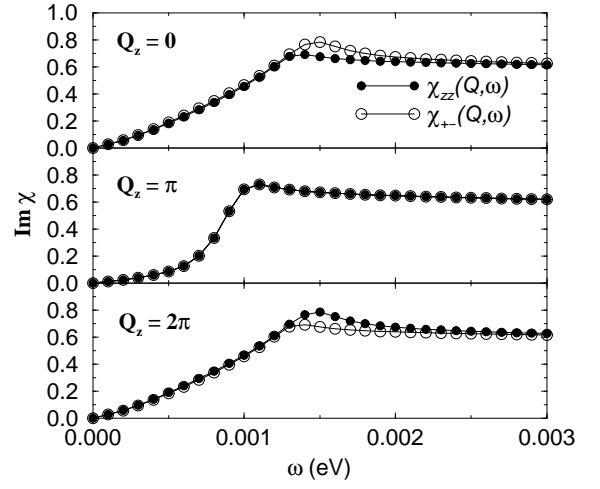


FIG. 9: Imaginary part of the dynamical susceptibility in the case C (line nodes on one-dimensional Fermi surface, eq. (32)) calculated in RPA. We take the same parameters as in Fig. 3.

### IV. COMPARISON WITH SPIN-SINGLET SUPERCONDUCTIVITY

Eq. (11) can be also applied for the spin-singlet case, when the order parameter is written as  $\Delta_{\alpha\beta}(\mathbf{k}) = i\sigma_{\alpha\beta}^y \Delta(\mathbf{k})$ . As expected, we get the isotropic coherence factor

$$\begin{aligned} &\sum_{\alpha\alpha'\beta\beta'} \sigma_{\alpha\alpha'}^i \sigma_{\beta\beta'}^j C_{\alpha\alpha'\beta\beta'}^{(\pm)} \\ &= \delta_{ij} \left( 1 \pm \frac{\xi_{\mathbf{k}} \xi_{\mathbf{k}'} + \text{Re}(\Delta^*(\mathbf{k})\Delta(\mathbf{k}'))}{E_{\mathbf{k}} E_{\mathbf{k}'}} \right). \end{aligned} \quad (34)$$

A peak appears in  $\text{Im}\chi_{ii}(\mathbf{q}, \omega)$ , only if  $\text{Re}(\Delta^*(\mathbf{k})\Delta(\mathbf{k}')) < 0$ , which is the case for the  $d$ -wave paring with  $\mathbf{q} \approx (\pi, \pi, q_z)$  in high  $T_c$  cuprates<sup>24,27,30,33,36,45</sup>. Note that the dynamical spin-susceptibility  $\chi_{+-}(\mathbf{q}, \omega)$  (eq. (15)) for the spin-triplet superconductivity is similar to the dynamical *charge*-susceptibility in the spin-singlet superconductivity<sup>46</sup>.

### V. CONCLUSION

We study the dynamical spin-susceptibility for the spin-triplet superconductivity. The resonance peak appears either in  $\text{Im}\chi_{zz}(\mathbf{q}, \omega)$  or  $\text{Im}\chi_{+-}(\mathbf{q}, \omega)$  from the nesting part of the Fermi surface. We have shown that the existence of the line nodes on the quasi-one dimensional Fermi surface drastically changes the dynamical susceptibility, which can be observed by inelastic neutron scattering experiments.

Coherence peak appears in  $\text{Im}\chi_{+-}(\mathbf{Q}, \omega)$  if  $\text{Re}(d_z^*(\mathbf{k})d_z(\mathbf{k} + \mathbf{Q})) > 0$  or in  $\text{Im}\chi_{zz}(\mathbf{Q}, \omega)$  if  $\text{Re}(d_z^*(\mathbf{k})d_z(\mathbf{k} + \mathbf{Q})) < 0$ . When  $\text{Re}(d_z^*(\mathbf{k})d_z(\mathbf{k} + \mathbf{Q}))$  changes sign in the nested part of the Fermi surface,

a coherence peak can appear in both  $\text{Im}\chi_{zz}(\mathbf{Q},\omega)$  and  $\text{Im}\chi_{+-}(\mathbf{Q},\omega)$ , but the divergence becomes weaker and easily smeared out. The position of the line nodes on the Fermi surface, if line nodes exist in the nested part of the Fermi surface, will be observed by scanning  $Q_z$  in the inelastic neutron scattering.

Recently, the resonance peak was searched in  $\text{Sr}_2\text{RuO}_4$  by inelastic neutron scattering<sup>43,44</sup>, but no changes have been observed below  $T_c$  yet. We take the amplitude of the order parameter in the one-dimensional band as

$\Delta_1 = 0.001$  eV in the RPA calculation. If the one-dimensional band is passive, the value may be smaller and the observation will be difficult. The gap structure, however, will be observed by experiments with better resolutions using better single crystals.

Recently, Mukuda et al<sup>47</sup> reported a different dependence of the relaxation in Ruthenium and Oxide nuclear quadrupole resonance. This difference may be explained by the difference of  $\chi_{+-}(\mathbf{q},\omega)$  and  $\chi_{zz}(\mathbf{q},\omega)$  in the spin triplet superconductivity.

- 
- <sup>1</sup> Y. Maeno et al. Y. Maeno, H. Hashimoto, K. Yoshida, S. Nishizaki, T. Fujita, J.G. Bednorz, and F. Lichtenberg, *Nature (London)* **372**, 532 (1994).
  - <sup>2</sup> K. Ishida, H. Mukuda, Y. Kitaoka, K. Asayama, Z. Q. Mao, Y. Mori and Y. Maeno, *Nature (London)* **396**, 658 (1998).
  - <sup>3</sup> J. A. Duffy, S. M. Hayden, Y. Maeno, Z. Mao, J. Kulda, and G. J. McIntyre, *Phys. Rev. Lett.* **85**, 5412, (2000).
  - <sup>4</sup> G. M. Luke, Y. Fudamoto, K. M. Kojima, M. I. Larkin, J. Merrin, B. Nachumi, Y. J. Uemura, Y. Maeno, Z. Q. Mao, Y. Mori, H. Nakamura, and M. Sigrist, *Nature (London)* **394**, 558 (1998).
  - <sup>5</sup> K. Ishida, H. Mukuda, Y. Kitaoka, Z. Q. Mao, Y. Mori, and Y. Maeno *Phys. Rev. Lett.* **84**, 5387 (2000).
  - <sup>6</sup> S. NishiZaki et al., S. NishiZaki, Y. Maeno and Z. Q. Mao, *J. Phys. Soc. Jpn.* **69**, 572 (2000).
  - <sup>7</sup> C. Lupien, W. A. MacFarlane, Cyril Proust, and Louis Taillefer *Phys. Rev. Lett.* **86**, 5986 (2001).
  - <sup>8</sup> M. Suzuki, M. A. Tanatar, N. Kikugawa, Z. Q. Mao, Y. Maeno, and T. Ishiguro, *Phys. Rev. Lett.* **88**, 227004 (2002).
  - <sup>9</sup> Y. Hasegawa, K. Machida, and M. Ozaki, *J. Phys. Soc. Jpn.* **69**, 336 (2000).
  - <sup>10</sup> K. Izawa, H. Takahashi, H. Yamaguchi, Y. Matsuda, M. Suzuki, T. Sasaki, T. Fukase, Y. Yoshida, R. Settai, and Y. Onuki, *Phys. Rev. Lett.* **86**, 2653 (2001).
  - <sup>11</sup> M. A. Tanatar, M. Suzuki, S. Nagai, Z. Q. Mao, Y. Maeno, and T. Ishiguro, *Phys. Rev. Lett.* **86**, 2649 (2001).
  - <sup>12</sup> A. P. Mackenzie, S. R. Julian, A. J. Diver, G. J. McMullan, M. P. Ray, G. G. Lonzarich, Y. Maeno, S. Nishizaki, and T. Fujita, *Phys. Rev. Lett.* **76**, 3786 (1996).
  - <sup>13</sup> A. Damascelli et al., A. Damascelli, D. H. Lu, K. M. Shen, N. P. Armitage, F. Ronning, D. L. Feng, C. Kim, and Z.-X. Shen, T. Kimura and Y. Tokura, Z. Q. Mao, and Y. Maeno *Phys. Rev. Lett.* **85**, 5194 (2000).
  - <sup>14</sup> T. Oguchi, *Phys. Rev. B* **51**, 1385 (1995).
  - <sup>15</sup> D. J. Singh, *Phys. Rev. B* **52**, 1358 (1995).
  - <sup>16</sup> I. I. Mazin and D. J. Singh, *Phys. Rev. Lett.* **82**, 4324 (1999).
  - <sup>17</sup> Y. Sidis, M. Braden, P. Bourges, B. Hennion, S. NishiZaki, Y. Maeno, and Y. Mori, *Phys. Rev. Lett.* **83**, 3320 (1999).
  - <sup>18</sup> M. E. Zhitomirsky and T. M. Rice, *Phys. Rev. Lett.* **87**, 057001 (2001).
  - <sup>19</sup> T. Nomura and K. Yamada, *J. Phys. Soc. Jpn.* **71**, 404 (2002).
  - <sup>20</sup> M. Sato and M. Kohmoto, *J. Phys. Soc. Jpn.* **69**, 3505 (2000).
  - <sup>21</sup> T. Kuwabara and M. Ogata, *Phys. Rev. Lett.* **85**, 4586 (2000).
  - <sup>22</sup> J. Rossat-Mignod, L.P. Regnault, C. Vettier, P. Bourges, P. Burllet, J. Rossy, J.Y. Henry and G. Lapertot, *Physica C* **185-189**, 86 (1991).
  - <sup>23</sup> H.A. Mook, M. Yethiraj, G. Aeppli, T.E. Mason and T. Armstrong, *Phys. Rev. Lett.* **70**, 3490 (1993)
  - <sup>24</sup> H.F. Fong, B. Keimer, P.W. Anderson, D. Reznik, F. Dogan and I. A. Aksay, *Phys. Rev. Lett.* **75**, 316 (1995).
  - <sup>25</sup> P. Bourges, L.P. Regnault, Y. Sidis and C. Vettier, *Phys. Rev. B.* **53**, 876 (1996).
  - <sup>26</sup> P. Dai, H.A. Mook, R. D. Hunt, and F. Dogan, *Phys. Rev. B* **63**, 054525 (2001),
  - <sup>27</sup> J.P. Lu, *Phys. Rev. Lett.* **68**, 125 (1992).
  - <sup>28</sup> N. Bulut and D. J. Scalapino, *Phys. Rev. B.* **47**, 3419, (1993).
  - <sup>29</sup> T. Tanamoto, H. Kohno, and H. Fukuyama, *J. Phys. Soc. Jpn.* **62**, 1455 (1993).
  - <sup>30</sup> T. Tanamoto, H. Kohno, and H. Fukuyama, *J. Phys. Soc. Jpn.* **63**, 2739 (1994).
  - <sup>31</sup> F. Marsiglio, *Phys. Rev. B* **47**, 11555 (1993).
  - <sup>32</sup> M. Lavagna and G. Stemann, *Phys. Rev. B* **49**, 4235 (1994).
  - <sup>33</sup> K. Maki and H. Won, *Phys. Rev. Lett.* **72**, 1758 (1994).
  - <sup>34</sup> E. Demler and S. C. Zhang, *Phys. Rev. Lett.* **75**, 4126 (1995).
  - <sup>35</sup> D.Z. Liu and Y. Zha and K. Levin, *Phys. Rev. Lett.* **75**, 4130 (1995).
  - <sup>36</sup> I.I. Mazin and V.M. Yakovenko, *Phys. Rev. Lett.* **75**, 4134 (1995).
  - <sup>37</sup> J. Brinckmann and P.A. Lee, *Phys. Rev. Lett.* **82**, 2915 (1999).
  - <sup>38</sup> W.F. Brinkman, J. W. Serene, and P. W. Anderson, *Phys. Rev. A* **10**, 2386 (1974).
  - <sup>39</sup> R. Joynt and T.M. Rice, *Phys. Rev. B* **38**, 2345 (1988).
  - <sup>40</sup> D. K. Morr, P. F. Trautman, and M. J. Graf, *Phys. Rev. Lett.* **86**, 5978 (2001).
  - <sup>41</sup> H. Y. Kee, *J. Phys. Condens. Matter* **12**, 2279 (2000).
  - <sup>42</sup> D. Fay and L. Tewordt, *Phys. Rev. B* **62**, 4036 (2000).
  - <sup>43</sup> F. Servant et al., *Phys. Rev. B* **65**, 184511 (2002).
  - <sup>44</sup> M. Braden et al. *Phys. Rev. B.* **66**, 064522 (2002).
  - <sup>45</sup> M. Lavagna and G. Stemann, *Phys. Rev. B* **49**, 4235 (1994).
  - <sup>46</sup> F. Marsiglio, *Phys. Rev. B* **47**, 5419 (1993).
  - <sup>47</sup> H. Mukuda, K. Ishida, Y. Kitaoka, K. Miyake, Z. Q. Mao, Y. Mori, and Y. Maeno *Phys. Rev. B* **65**, 132507 (2002)